The iron–sulfur cluster assembly (ISC) protein Iba57 executes a tetrahydrofolate-independent function in mitochondrial [4Fe–4S] protein maturation

Received for publication, June 3, 2022, and in revised form, August 23, 2022 Published, Papers in Press, September 6, 2022,
https://doi.org/10.1016/j.jbc.2022.102465

Ulrich Mühlenhoff[1,2,*], Benjamin Dennis Weiler[1], Franziska Nadler[1], Robert Millar[2], Isabell Kothe[1,2], Sven-Andreas Freibert[1,2], Florian Altegoer[2,3], Gert Bange[2,3], and Roland Lill[1,2,*]

From the [1]Institut für Zytobiologie im Zentrum SYNMIKRO, Philipps-Universität Marburg, Marburg, Germany; [2]Zentrum für Synthetische Mikrobiologie SynMikro, Marburg, Germany; [3]Fachbereich Chemie, Philipps-Universität Marburg, Marburg, Germany

Edited by Ruma Banerjee

Mitochondria harbor the bacteria-inherited iron–sulfur cluster assembly (ISC) machinery to generate [2Fe–2S; iron–sulfur (Fe–S)] and [4Fe–4S] proteins. In yeast, assembly of [4Fe–4S] proteins specifically involves the ISC proteins Isa1, Isa2, Iba57, Bol3, and Nfu1. Functional defects in their human equivalents cause the multiple mitochondrial dysfunction syndromes, severe disorders with a broad clinical spectrum. The bacterial Iba57 ancestor YgfZ was described to require tetrahydrofolate (THF) for its function in the maturation of selected [4Fe–4S] proteins. Both YgfZ and Iba57 are structurally related to an enzyme family catalyzing THF-dependent one-carbon transfer reactions including GcvT of the glycine cleavage system. On this basis, a universally conserved folate requirement in ISC-dependent [4Fe–4S] protein biogenesis was proposed. To test this idea for mitochondrial Iba57, we performed genetic and biochemical studies in *Saccharomyces cerevisiae*, and we solved the crystal structure of Iba57 from the thermophilic fungus *Chaetomium thermophilum*. We provide three lines of evidence for the THF independence of the Iba57-catalyzed [4Fe–4S] protein assembly pathway. First, yeast mutants lacking folate show no defect in mitochondrial [4Fe–4S] protein maturation. Second, the 3D structure of Iba57 lacks many of the side-chain contacts to THF as defined in GcvT, and the THF-binding pocket is constricted. Third, mutations in conserved Iba57 residues that are essential for THF-dependent catalysis in GcvT do not impair Iba57 function *in vivo*, in contrast to an exchange of the invariant, surface-exposed cysteine residue. We conclude that mitochondrial Iba57, despite structural similarities to both YgfZ and THF-binding proteins, does not utilize folate for its function.

Proteins with iron–sulfur (Fe–S) cofactors play important roles in fundamental cellular processes, including redox reactions, catalysis, translation, DNA synthesis and repair, antiviral defense, and the sensing of environmental conditions (1). The biogenesis of Fe–S proteins in all kingdoms of life is catalyzed by complex and conserved assembly systems (2–7). In eukaryotes including humans, maturation is initiated in mitochondria by the iron–sulfur cluster assembly (ISC) machinery, which comprises 18 known proteins, mostly of bacterial origin (8). Biosynthesis of cytosolic and nuclear Fe–S proteins further requires the mitochondrial ABC transporter Atm1 and the cytosolic Fe–S protein assembly system (9).

The assembly of Fe–S proteins by mitochondrial and related bacterial ISC systems occurs in four consecutive stages. First, a [2Fe–2S] cluster is formed *de novo* on the scaffold protein Isu1. In this multistep reaction, sulfur is initially released from free cysteine by the cysteine desulfurase complex Nfs1–Isd11–Acp1 and transferred to Fe-binding Isu1 in form of a persulfide, a reaction stimulated by frataxin (10–13). Next, the Isu1-bound persulfide is reduced to sulfide by electron input from the mitochondrial [2Fe–2S] ferredoxin Yah1 (8, 11, 13–16). *De novo* synthesis of the [2Fe–2S] cluster is facilitated by Isu1 dimerization induced by a conserved N-terminal tyrosine (16). In the second stage, target [2Fe–2S] protein assembly is initiated by cluster transfer from Isu1 to the monothiol glutaredoxin Grx5, a reaction assisted by the dedicated Hsp70 chaperone Ssq1 and its J-type cochaperone, Jac1 (3, 17–20). The transiently Grx5-bound [2Fe–2S] cluster is then passed on to target apoproteins without further ISC protein assistance (21–24).

In the third stage, mitochondrial [4Fe–4S] clusters are synthesized relying on a number of ISC proteins that are not involved in the first two stages. Initially, Grx5-bound [2Fe–2S] clusters are transferred to the A-type ISC proteins Isa1–Isa2 (24–33). As shown *in vitro* with the related human ISC proteins, two ISCA1–ISCA2-bound [2Fe–2S] clusters are reductively fused to a [4Fe–4S] cluster by electron transfer from the ferredoxin FDX2 and its NADPH-coupled reductase FDXR (24, 29). The reaction essentially requires the presence of IBA57, yet its mechanistic role remains ill defined. The intimate and conserved cooperation of the Isa1, Isa2, and Iba57

* For correspondence: Ulrich Mühlenhoff, muehlenh@staff.uni-marburg.de; Roland Lill, lill@staff.uni-marburg.de.
Present address for Franziska Nadler: University Medical Center Göttingen, Department of Cellular Biochemistry, Göttingen, Germany
Present address for Robert Millar: Department of Chemistry, University of Warwick, Coventry, UK
Present address for Florian Altegoer: Heinrich-Heine Universität Düsseldorf, Institut für Mikrobiologie, Universitätsstraße 1, Düsseldorf, Germany

proteins is supported by *in vivo* studies showing that deficiencies in these proteins in yeast or human cells elicit virtually identical phenotypes originating from a general mitochondrial [4Fe–4S] protein deficiency (25, 26, 28). In the fourth and final stage, the assembly of [4Fe–4S] target proteins such as respiratory complexes I and II or lipoyl synthase is assisted by additional dedicated ISC targeting factors, such as Ind1, Nfu1, or the BOLA family proteins Bol1–Bol3 (21, 34–36). Despite not being essential for yeast viability, mutations in these human late-acting ISC factors cause severe often lethal disorders including the "multiple mitochondrial dysfunction syndromes" with a wide phenotypical spectrum (37–43). Biochemically, these diseases are characterized by general defects in mitochondrial [4Fe–4S] proteins.

Iba57 and its bacterial homolog YgfZ belong to the COG0354 protein family of potential tetrahydrofolate (THF)-binding proteins with structural similarities to the T-subunit GcvT of the glycine cleavage system (31, 44). *Escherichia coli* YgfZ (EcYgfZ) binds folate derivatives *in vitro*, and both *ygfZ* deletion and ablation of folate biosynthesis are associated with diminished functions of a small subset of [4Fe–4S] proteins (44–47). Since mitochondrial Iba57 proteins from various organisms rescue the phenotype of EcYgfZ-deficient *E. coli* cells, a conserved role of folate was postulated for mitochondrial [4Fe–4S] protein formation (45). However, an experimental verification of this idea in eukaryotes is pending (48). In this work, we have used genetic, biochemical, and structural methods to investigate the potential role of folates in mitochondrial Iba57 function. We provide several lines of functional evidence that Iba57-assisted mitochondrial [4Fe–4S] protein maturation occurs independently of folates. This notion is supported by the 3D structure of mitochondrial Iba57 that is incompatible with high-affinity THF binding as found in GcvT.

Results

Folate is not required for Fe–S protein maturation in yeast

Based on studies with EcYgfZ, a universal role for THFs in the formation of iron-sulfur clusters was postulated (45). In *Saccharomyces cerevisiae*, mutants with defects in folate biosynthesis are viable when supplemented with adenine, His, Met, and deoxythymidine monophosphate (dTMP) (49–51). However, of these four folate-requiring supplements, only the biosynthesis of methionine involves iron-sulfur cluster-dependent enzymes, yet the specific folate-requiring step does not involve Fe–S proteins (48). In contrast, deletion of the *ygfZ* homolog *IBA57* in *S. cerevisiae* is associated with auxotrophies for Glu and Lys that are caused by loss of function of the mitochondrial [4Fe–4S] proteins aconitase and homoaconitase, respectively (25). These auxotrophies were not reported previously for any folate biosynthesis mutant in *S. cerevisiae*, which puts the postulated role of THF in the enzymatic activity of mitochondrial Iba57 into question (49–51).

In order to resolve this point, we analyzed yeast strains with defects in THF biosynthesis and/or utilization for potential defects in mitochondrial Fe–S protein maturation. First, we chose four mutants with gene deletions of key components of mitochondrial THF metabolism: Met13, the mitochondrial methylenetetrahydrofolate reductase; Met7, the folylpolyglutamate synthetase required for methionine synthesis and mitochondrial DNA maintenance (52); Mis1, the mitochondrial C1-THF synthase; and Ade3, the cytosolic counterpart of Mis1. Furthermore, we created an *ade3*Δ/*mis1*Δ double mutant that is unable to produce 5,10-methenyltetrahydrofolate (50, 51). Yet, despite their strong defects in one-carbon metabolism, all these mutants were perfectly able to grow on minimal medium lacking Lys and Glu, clearly differing from an aconitase (Aco1) deletion mutant (Fig. 1*A*). Next, we analyzed yeast mutants deleted for *FOL2* encoding the GTP-cyclohydrolase I that catalyzes the first step in folate biosynthesis (53, 54). We created two *fol2*Δ strains by independent deletion strategies in order to ensure that the observed phenotypes were not because of secondary effects caused by this massive impact in metabolism. Both mutants were unable to grow in rich or minimal medium lacking folate, unless supplemented with the four folate-requiring supplements, in particular dTMP (Fig. 1*B* and Fig. S1*A*). Furthermore, the *fol2*Δ strains were unable to grow on the nonfermentable carbon source glycerol (Fig. S1*B*). Mating experiments with a rho^0 tester strain indicated the loss of mitochondrial DNA as a result of the *FOL2* deletion. However, unlike *iba57*Δ cells that are also rho^0, the *fol2*Δ strains did not require Lys or Glu for growth (Fig. 1*B*) (25). The slower growth of the *fol2*Δ mutants under this condition was likely because of their rho^0 phenotype (*cf.* Fig. S1*B*). Consistently, *fol2*Δ cells displayed wildtype aconitase activities (Fig. 1*C*), and the lipoylation of mitochondrial pyruvate- and α-ketoglutarate-dehydrogenase subunits Lat1 and Kgd2, respectively, was normal (Fig. 1*D*). Both aconitase and the radical-SAM enzyme lipoyl synthase (Lip5) are mitochondrial [4Fe–4S] proteins and essentially require Iba57 for maturation (25, 28). Taken together, these data show that folate, in contrast to Iba57, is not required for the biogenesis of mitochondrial [4Fe–4S] proteins.

In order to test whether the folate-dependent bacterial YgfZ can replace yeast Iba57 in mitochondrial Fe–S protein biogenesis, we expressed EcYgfZ with an N-terminal mitochondrial targeting sequence in *iba57*Δ cells. However, these transformed cells remained unable to grow on minimal medium lacking Lys and Glu, and aconitase activities were not restored, even when EcYgfZ was overproduced from a p424 high-copy vector (Fig. 2, *A* and *B*). This did not change when *E. coli* IscA, a likely partner of EcYgfZ, was coexpressed together with EcYgfZ. The localization of EcYgfZ in mitochondria of *iba57*Δ cells was verified by expressing EcYgfZ with a C-terminal Myc tag from low- (p416) or high-copy (p426) vectors (Fig. 2*C*). Like EcYgfZ, EcYgfZ-Myc also did not rescue the growth defect of *iba57*Δ cells (Fig. S2). Apparently, EcYgfZ cannot replace Iba57 in yeast, although vice versa yeast Iba57 can substitute EcYgfZ in *E. coli*, albeit poorly (45). This observation is reminiscent of complementation studies with the plastid version of *Arabidopsis thaliana* IBA57, which could functionally replace EcYgfZ in *E. coli* but not Iba57 in yeast (45, 55).

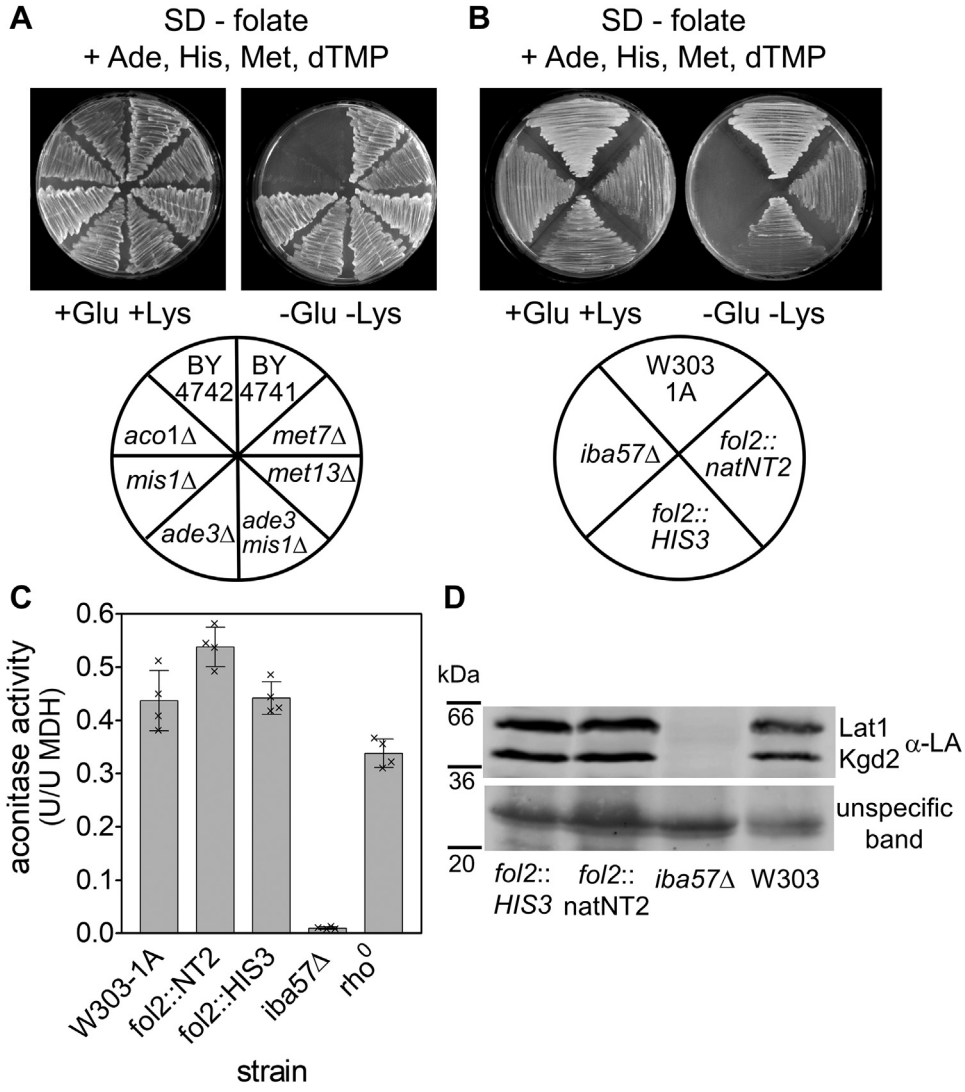

Figure 1. Folate is not required for mitochondrial [4Fe–4S] protein biogenesis in *Saccharomyces cerevisiae*. *A,* the indicated yeast strains (BY4741 background; *MATa his3Δ leu2Δ met15Δ ura3Δ*) with defects in the utilization or modification of folate were cultivated on folate-free synthetic defined (SD) minimal medium containing the four folate-dependent supplements Ade, His, Met, and dTMP in the presence or the absence of Lys and Glu. BY4742 (*MATa his3Δ leu2Δ lys2Δ ura3Δ*) and *aco1Δ* (W303-1A background) requiring supplementation with either Lys or Glu served as control. *B,* two independent folate-auxotroph *fol2Δ* deletion strains (W303-1A background) were streaked onto folate-free SD minimal medium agar plates plus Ade, His, Met, and dTMP in the presence or the absence of Lys and Glu. *C* and *D,* cells cultivated in folate-free SD minimal medium plus Ade, His, Met, and dTMP were assayed for (*C*) aconitase enzyme activities (relative to malate dehydrogenase [MDH]) in cell extracts and (*D*) the lipoylation (LA) of the E2 subunits of pyruvate (Lat1) and 2-ketoglutarate dehydrogenases (Kgd2) by immunostaining of isolated mitochondrial extracts. An unspecific band crossreacting with the anti-LA antibody served as a loading control. W303-1A wildtype and rho^0 cells as well as *iba57Δ* were used as controls. Error bars indicate the SD (n ≥ 4). dTMP, deoxythymidine monophosphate.

The 3D structure of mitochondrial Iba57 is incompatible with high-affinity THF binding

To obtain structural criteria for whether mitochondrial Iba57 might be a THF-dependent enzyme, we solved the crystal structure of Iba57 from the thermophilic fungus *Chaetomium thermophilum* (Ct). The mature form of CtIba57 (residues 61–476) was expressed in *E. coli* BL21 (DE3) and purified *via* an N-terminal His tag by nickel–nitrilotriacetic acid affinity and size-exclusion chromatography. The crystal structure of CtIba57 (Protein Data Bank [PDB] code: 7Z3H) was solved by molecular replacement using the structure of human Iba57 (HsIBA57) as a search model (Table S1) (31). Similar to EcYgfZ, CtIba57 crystallized as a disulfide-bridged homodimer (44) (Fig. 3*A*). Since the conserved Cys304 is essential for function in [4Fe–4S] cluster formation *in vitro* (24) (see also later), and since the interface area is rather small, the dimerization likely is a consequence of the long incubation time during crystallization. Each CtIba57 monomer consists of 9 α-helices and 16 β-strands forming three domains (1–3) (Fig. 3*B*). Domains 1 (residues 90–192) and 2 (residues 73–89 and 195–248) are separated from domain 3 (residues 310–422) by three α-helices that wrap the entire protein (α4, α6, and α9). Superposition analysis with the structures of the human ortholog HsIBA57 (PDB code: 6QE4), the *E. coli* homolog EcYgfZ (PDB code: 1NRK), and the T-subunit HsGcvT (aka GCST) of the human mitochondrial glycine cleavage complex

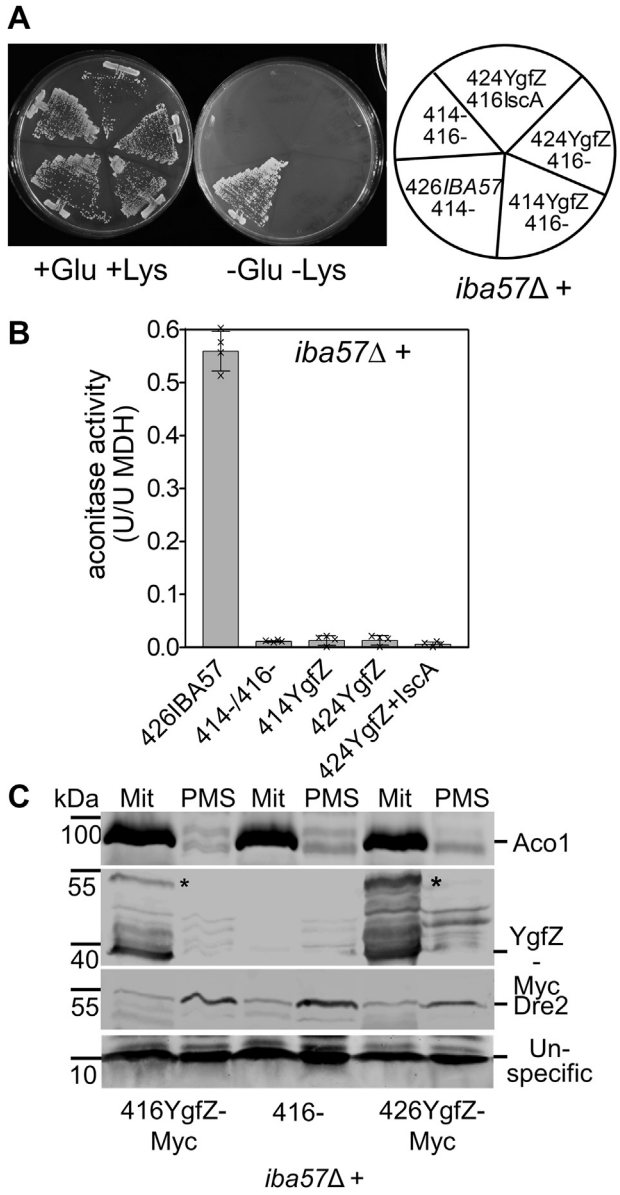

Figure 2. *Escherichia coli YgfZ* does not complement *Saccharomyces cerevisiae iba57Δ* cells. *A,* strain *iba57*Δ (W303-1A background) was transformed with the indicated combinations of plasmids (Table S3) that allow the expression of *E. coli* YgfZ and IscA in mitochondria under the control of the *TDH3* promoter. Cells were cultivated on synthetic defined (SD) minimal medium agar plates in the presence or the absence of Lys and Glu. *B,* cells were cultivated in SD minimal medium, and cell extracts were assayed for aconitase activities. *iba57*Δ expressing yeast *IBA57* from a plasmid and cells with empty vector served as controls. Error bars indicate the standard deviation (n ≥ 4). *C, iba57*Δ cells harboring low-copy (p416) or high-copy (p426) vectors for the expression of EcYgfZ with a C-terminal Myc tag under the control of the *TDH3* promoter were fractionated into mitochondria (Mit) and postmitochondrial supernatant (PMS) fractions. *iba57*Δ cells with the empty vector (p416) served as a control. Fractions were analyzed for the presence of EcYgfZ by immunostaining with α-Myc antibodies. The *asterisks* (*) likely indicate the noncleaved EcYgfZ-Myc precursor. Stains for mitochondrial Aco1 and cytosolic Dre2 serve to document the quality of the fractionation. An unspecific protein stained with Fast Green FCF served as a loading control. EcYgfZ, *Escherichia coli* YgfZ.

(PDB code: 1WSV) showed an overall low rmsd of 1.012 over 204 C^{α} atoms, 1.106 over 120 C^{α} atoms, and 1.230 over 87 C^{α} atoms, respectively (Fig. 3*C*). Despite the overall low primary sequence conservation, the structures of the two mitochondrial Iba57 proteins are virtually identical, except for a short 25-residue long insertion present in CtIba57 (and other fungal relatives) in front of the conserved C-terminal PxW motif (Fig. S3*A*). Moreover, and of importance for our further study, the core regions of the Iba57 proteins display a high structural similarity with both EcYgfZ and HsGcvT.

Reminiscent of the EcYgfZ and HsIBA57 structures, we did not detect any THF or related folates within the crystallized CtIba57. To gain structural insights into potential THF binding to Iba57 and YgfZ proteins, we compared the THF-binding region of HsGcvT with the respective areas in the Iba57–YgfZ structures (56). The glycine cleavage complex catalyzes the oxidative decarboxylation of glycine required for the formation of 5,10-methylene-THF (57, 58). Its T-subunit GcvT is a THF-dependent amino methyltransferase that catalyzes the transfer of a methylene one-carbon unit to THF from a methylamine group at the lipoyl arm of the H-subunit GCSH of the glycine cleavage complex. In GcvT enzymes, THF binds in a central binding cleft formed by the two N-terminal domains of the protein with the pteridine ring being buried in a hydrophobic pocket and its glutamyl group pointing outward (Fig. 3*C*, *right*; enlargement in Fig. 4*A*) (56, 59–61). Superposition of HsGcvT and CtIba57 shows that the CtIba57 loop connecting β9 and β10 strands from domain 2 (β9–10-loop) and the loop adjacent to α5 (α5-loop) are shifted toward each other (Fig. 4*A*; *blue arrows*). As a consequence, the potential entry tunnel to the pteridine pocket is virtually closed in CtIba57. This scenario also holds true for HsIBA57 and for the α5-loop of EcYgfZ (Fig. S4). In addition, the entire THF-binding pocket as found in HsGcvT is almost completely filled in Iba57 proteins, because the side chains of the two loops protrude into this pocket (Figs. 4*B* and 5, *A* and *B*).

In HsGcvT, several residues are involved in THF binding. In particular, Met56, Asp101, Tyr197, Glu204, and R233 of HsGcvT (PDB code: 1WSV; residues highlighted in *yellow* in Fig. S3) make contacts with THF. The first four residues are invariant in THF-binding family proteins such as HsGcvT homologs, the guanine nucleotide-binding protein TrmE (PDB code: 1XZQ), and dimethylglycine oxidase DMGO (PDB code: 1PJ6), and define the canonical THF-binding residues (56, 62–64) (Fig. 4*C*, *left panel*). R233 is specific for GcvT proteins. While in HsGcvT, Met56 and Tyr197 form the hydrophobic pocket for the pteridine group, the side chain of Glu204 undergoes a double hydrogen bonding toward the amino group bound to the C2 position and the N3 of the pteridine ring (56, 59, 60). In one-carbon transfer, Asp101 assists the nucleophilic attack of the catalytic N10 group of THF on the methylene carbon on the GCSH-bound lipoyl arm by proton abstraction (58, 62, 64).

In CtIba57, the positively charged Arg90 replaces the hydrophobic Met56 of HsGcvT (residues Arg56 in HsIBA57 and Trp27 in EcYgfZ), and the position occupied by Tyr197 in HsGcvT does not exist, neither in any of the Iba57 proteins nor in EcYgfZ (Fig. 4*C*, *right panel*; Fig. S3, highlighted in *yellow*). These differences fully abolished the hydrophobic cavity accommodating the pteridine group of THF in HsGcvT. The negatively charged Glu204 in HsGcvT is replaced by

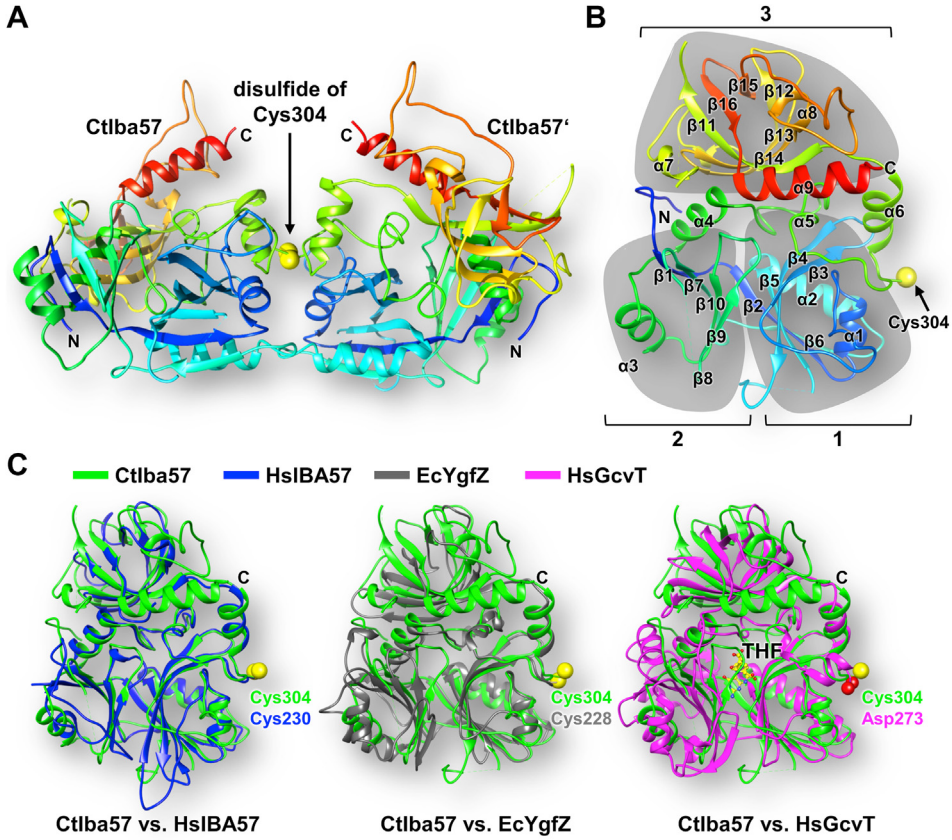

Figure 3. Crystal structure of *Chaetomium thermophilum* Iba57 at 2.4 Å resolution. *A,* disulfide-bridged (*via* Cys304) dimer of Ctlba57 as found in the crystal. Residues are *rainbow* colored from N (*blue*) to C termini (*red*). *B, cartoon* representation of Ctlba57 monomer (coloring as in *A*). The three individual domains are highlighted in *gray* (1–3). The sulfur of the essential Cys304 is depicted as a *yellow sphere*. *C,* superposition of Ctlba57 (*green*) with HsIBA57 (*blue*, *left*; Protein Data Bank [PDB] code: 6QE4), EcYgfZ (*gray*, *middle*; PDB code: 1NRK), and HsGcvT (*magenta*, *right*; PDB code: 1WSV). The conserved Cys residues of Iba57 (Ct and Hs) and EcYgfZ as well as the structural equivalent Asp273 of HsGcvT are depicted as *spheres*. THF of HsGcvT is shown in *yellow* (for enlargement, see Fig. 4*A*). Ctlba57, Ctlba57, *Chaetomium thermophilum* Iba57; EcYgfZ, *Escherichia coli* YgfZ; HsGcvT, human GcvT; HsIBA57, human IBA57; THF, tetrahydrofolate.

hydrophobic residues in CtIba57 (Ile236), HsIBA57 (Leu198), and EcYgfZ (Ile163), thus preventing hydrogen bonding to the pteridine ring. Interestingly, the invariant and catalytically important residue Asp101 of HsGcvT was retained in CtIba57 (Asp141), HsIBA57 (Asp109), and in most bacterial YgfZ proteins (Fig. 4*C*, *right panel*; Fig. S3, highlighted in *yellow*). As an exception to most bacterial YgfZ members, EcYgfZ carries an Asn at this position (Asn72).

We finally investigated the crystal structures of CtIba57, HsIBA57, and EcYgfZ for the presence of potential cavities as seen in HsGcvT for the lipoyl entry tunnel and the THF-binding pocket (calculated by PyMOL 2.0; Schrödinger, LLC). We found significant differences (Fig. 5, *A* and *B*). While the mitochondrial Iba57 proteins completely lack the THF-binding pocket (Fig. 4*B*), they retain the entry tunnel of HsGcvT for the lipoyl arm of the GCSH subunit of the glycine cleavage system, although the respective residues are not conserved (Fig. S3*B*). Moreover, HsIBA57 and CtIba57 completely lack the positively charged patch located at the C terminus of HsGcvT that binds the polyglutamate tail of THF (56, 59, 60, 64) (Fig. 5*C*). In eukaryotes, folylpolyglutamylation significantly enhances the THF affinity for mitochondrial and cytosolic folate–dependent enzymes and is required for folate retention within the cell, particularly in mitochondria (52, 65, 66). Collectively, these structural considerations strongly suggest that mitochondrial Iba57 proteins appear to be unable to bind and utilize THF for enzymatic function. The situation seems only slightly different for EcYgfZ, where the THF-binding pocket appears to be partially retained, yet with an amino acid composition differing significantly from the canonical folate-binding site (Fig. 4*C*). Furthermore, the potential entrance for the lipoyl arm of GCSH is fully blocked in EcYgfZ, and the positively charged polyglutamate-binding patch of HsGcvT is poorly maintained. These substantial structural changes of EcYgfZ relative to HsGcvT explain well why only a low affinity binding of folates (millimolar range) was observed for EcYgfZ (45) (see also *Discussion* section). Taken together, the low sequence conservation and, more importantly, the drastic changes in the topology and biochemical environment of the HsGcvT-related THF-binding area render physiologically relevant THF binding to mitochondrial Iba57 proteins and in turn a THF-dependent function unlikely. Based on similar, yet characteristically different structural considerations, the same appears to be true for EcYgfZ.

Mutational analyses confirm the THF-independent function of Iba57

One of the few positions of primary sequence conservation between the Iba57–YgfZ and GcvT protein families is the

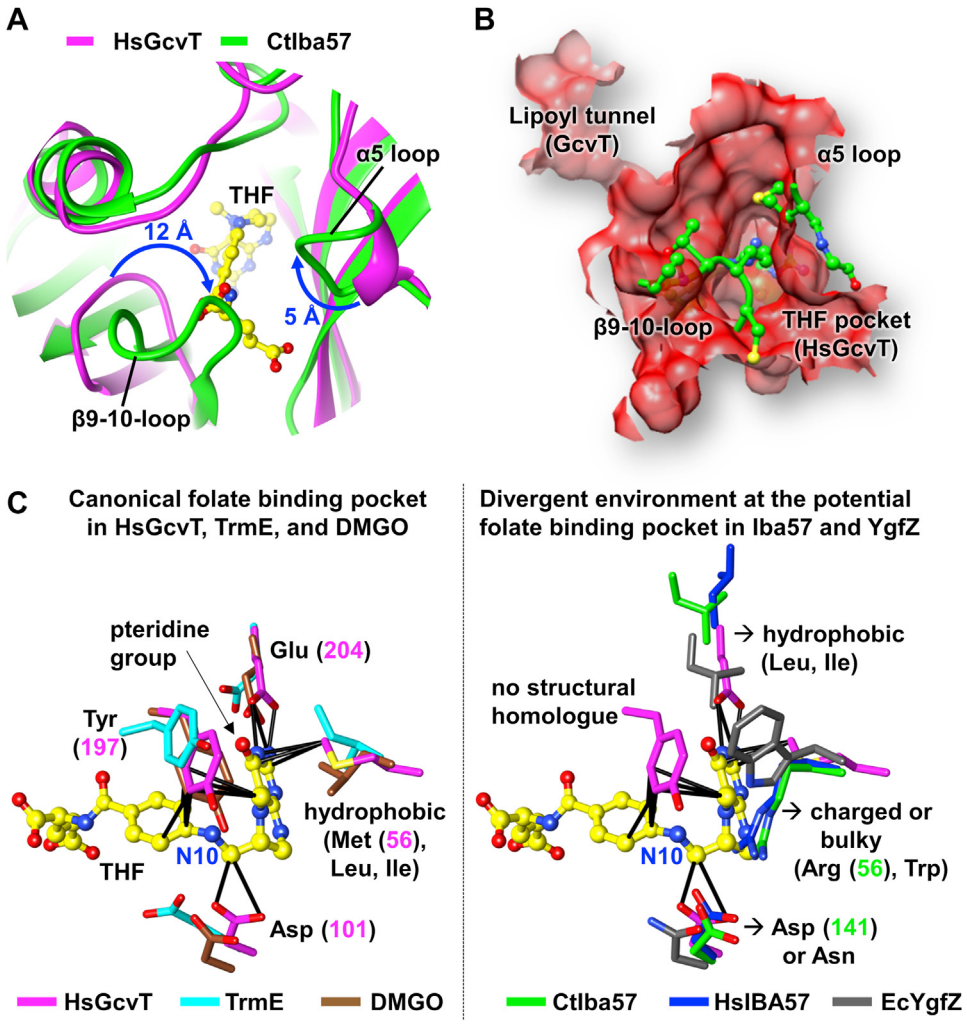

Figure 4. The structure of CtIba57 is incompatible with THF binding. *A,* superposition of CtIba57 (*green*) and HsGcvT (*magenta*; Protein Data Bank [PDB] code: 1WSV) highlighting the THF (*yellow*)-binding region of HsGcvT. The loops β9–10 and α5 that would interfere with THF binding in CtIba57 are marked. *Blue arrows* indicate the distances of the structural rearrangements of the respective loops. (For a comparison including HsIBA57 and EcYgfZ, refer to Fig. S4). *B,* the cavity of HsGcvT (*red*) encompassing its THF-binding site (THF pocket) and its lipoyl entrance tunnel was calculated using PyMOL. Side chains of residues in β9–10 and α5 loops of CtIba57 (*green*; shown as *balls and sticks*) protrude into the THF pocket of HsGcvT. *C,* comparison of residues involved in THF (*yellow*) binding to various proteins. *Left,* the canonical THF-binding pocket as found in HsGcvT (*magenta*), TrmE (*cyan*; PDB code: 1XZQ), and DMGO (*sienna*; PDB code: 1PJ6). The residue numbers are indicated in parenthesis for HsGcvT. *Right,* comparison of the THF-binding residues of HsGcvT (as shown *left*) with the structurally equivalent residues of CtIba57 (*green*), HsIBA57 (*blue*, PDB code: 6QE4), and EcYgfZ (*gray*, PDB code: 1NRK). The residue numbers are indicated in *parenthesis* for CtIba57. Only the side chains are depicted as *sticks*. Contacts are indicated by *black lines*. The catalytically important N10 position of THF is marked. CtIba57, *Chaetomium thermophilum* Iba57; EcYgfZ, *Escherichia coli* YgfZ; HsGcvT, human GcvT; HsIBA57, human IBA57; THF, tetrahydrofolate.

well-conserved Asp141 of CtIba57 that within HsGcvT (Asp101) assists the nucleophilic attack of the reactive N10 group of THF on the methylene carbon on the lipoyl arm (Fig. 4*C*; Fig. S3) (58, 62, 64). In HsGcvT, mutations of Asp101 to Asn or Ala are associated with a complete loss of function (56). As mentioned previously, in EcYgfZ, this residue is changed to Asn, further challenging the claim of a THF-dependent enzymatic function of EcYgfZ. Since the catalytic Asp101 of HsGcvT is conserved in mitochondrial Iba57 proteins, it serves as an excellent residue to test for potential THF-dependent catalytic function of Iba57. We employed yeast genetics and exchanged the corresponding Asp149 of *S. cerevisiae* Iba57 to Asn or Ala (*cf.* Fig. S3*A*). We further substituted residue Arg376, which is invariant in mitochondrial Iba57 proteins by His (Fig. S5). In HsGcvT, the corresponding residue Arg292 binds to the α-carboxylate group of THF and is conserved in eukaryotes. Its substitution by His results in decreased affinity to THF, loss of enzymatic activity, and causes nonketotic hyperglycinemia (48, 56, 67). Furthermore, we created a yeast mutant in which residues Arg366 and Arg374 of ScIba57 (Arg301 und Arg309 in CtIba57) were changed to Ala (termed R1,R2A). These residues are conserved in the Iba57–YgfZ family and might potentially contribute to a positively charged surface patch that in HsGcvT interacts with the polyglutamate moiety of folyl-polyglutamate, thereby stabilizing THF binding to HsGcvT (48, 64, 65, 68) (Fig. 5*C* and S3*A*). The corresponding ScIba57 variants were expressed from low-copy plasmids under the control of the endogenous promoter, and all perfectly rescued the Lys and Glu auxotrophy of *iba57*Δ yeast cells (Fig. 6*A*). As

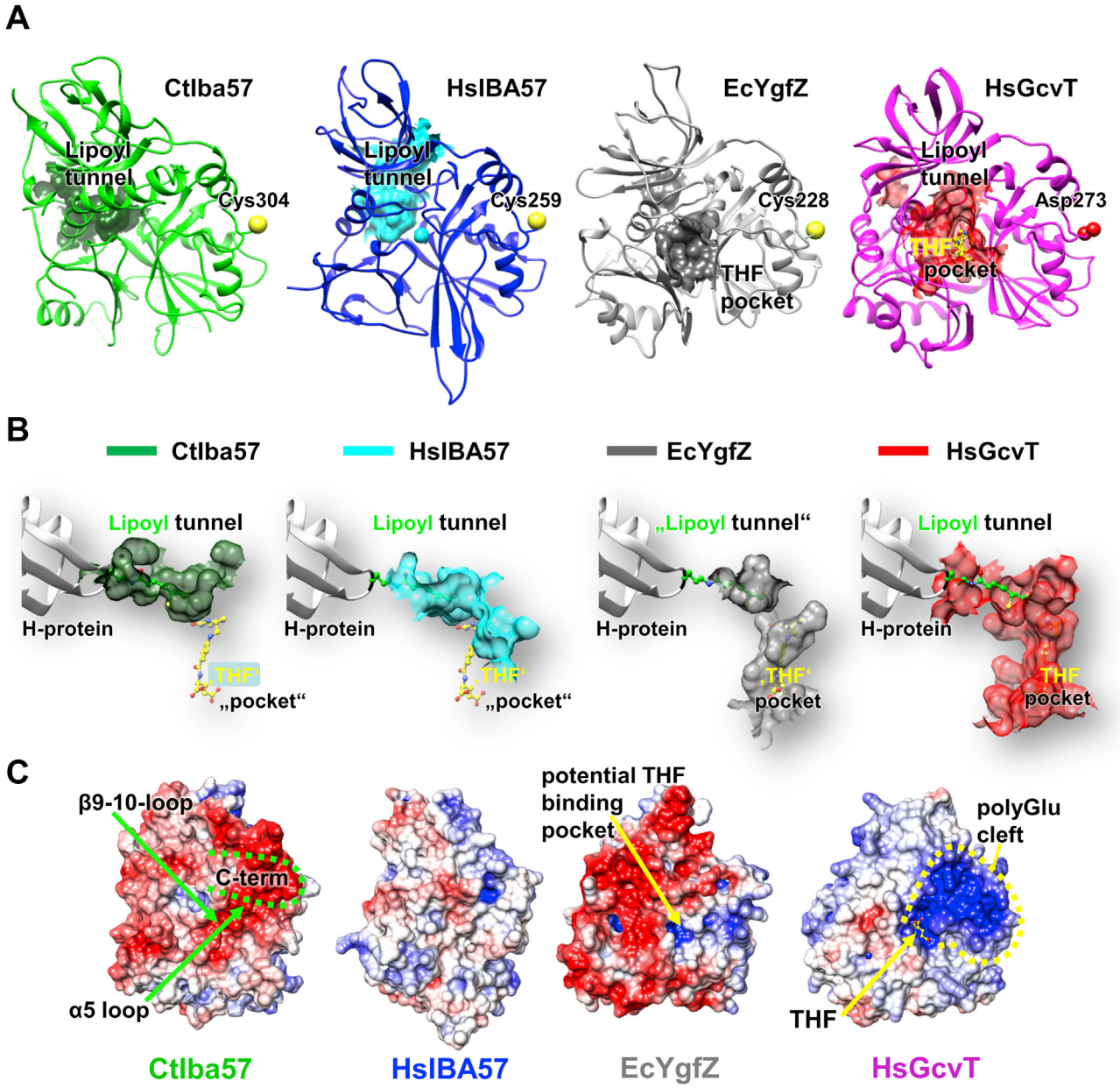

Figure 5. Cavities and surfaces of Iba57 and EcYgfZ exclude productive THF binding. *A,* cavities inside the *cartoon ribbon* representation were calculated for the indicated proteins using PyMOL. In HsGcvT, the cavity forms both the tunnel for the lipoyl arm of GCSH and the binding pocket for THF (*yellow*). *B,* the cavities extracted from *A* with attached human GCSH protein (location taken from the GCSH–HsGcvT complex (Protein Data Bank [PDB] code: 3A8I). The dihydrolipoyl moiety attached to GCSH protein is depicted in *light green*. THF (*yellow*) is shown as found in HsGcvT. *C,* surface charges (calculated by APBS biomolecular solvation software suite (80)) of the indicated proteins (*blue*: positive; *red*, negative). The β9–10- and α5-loops and the C terminus are indicated in CtIba57. The potential THF-binding pocket is indicated in EcYgfZ (*yellow arrow*). THF in HsGcvT is shown in *yellow,* and the poly-Glu binding site is outlined by a *yellow dotted line*. CtIba57, *Chaetomium thermophilum* Iba57; EcYgfZ, *Escherichia coli* YgfZ; HsGcvT, human GcvT; THF, tetrahydrofolate.

a control, we analyzed the *in vivo* consequences of exchanging the conserved surface-exposed Cys357 of the KGC(Y/F)XGQEL signature motif present in both mitochondrial Iba57 and bacterial YgfZ proteins (Fig. S3*A*). In *E. coli*, this residue is essential for EcYgfZ function *in vivo* (46, 69). Biochemical studies have shown a crucial function of this residue in HsIBA57 during the *in vitro* synthesis of [4Fe–4S] clusters (24). As expected from these studies, ScIba57–C357A and ScIba57–C357S variants were unable to rescue the Lys and Glu auxotrophy of *iba57*Δ cells, when expressed from low-copy plasmids under the control of the endogenous promoter (Fig. 6*A*), distinguishing this strong phenotype from the inconspicuous behavior of potential THF-binding residues of ScIba57.

We further analyzed the aforementioned mutants biochemically. In keeping with the growth phenotypes, *iba57*Δ cells expressing the potential THF-related ScIba57 variants showed wildtype aconitase activities, and the lipoylation of mitochondrial pyruvate and α-ketoglutarate dehydrogenase subunits was restored to wildtype levels (Fig. 6, *B–E*). In contrast, the two ScIba57–C357 variants did not show any aconitase or lipoylation activities. The same was seen when the C357S mutant

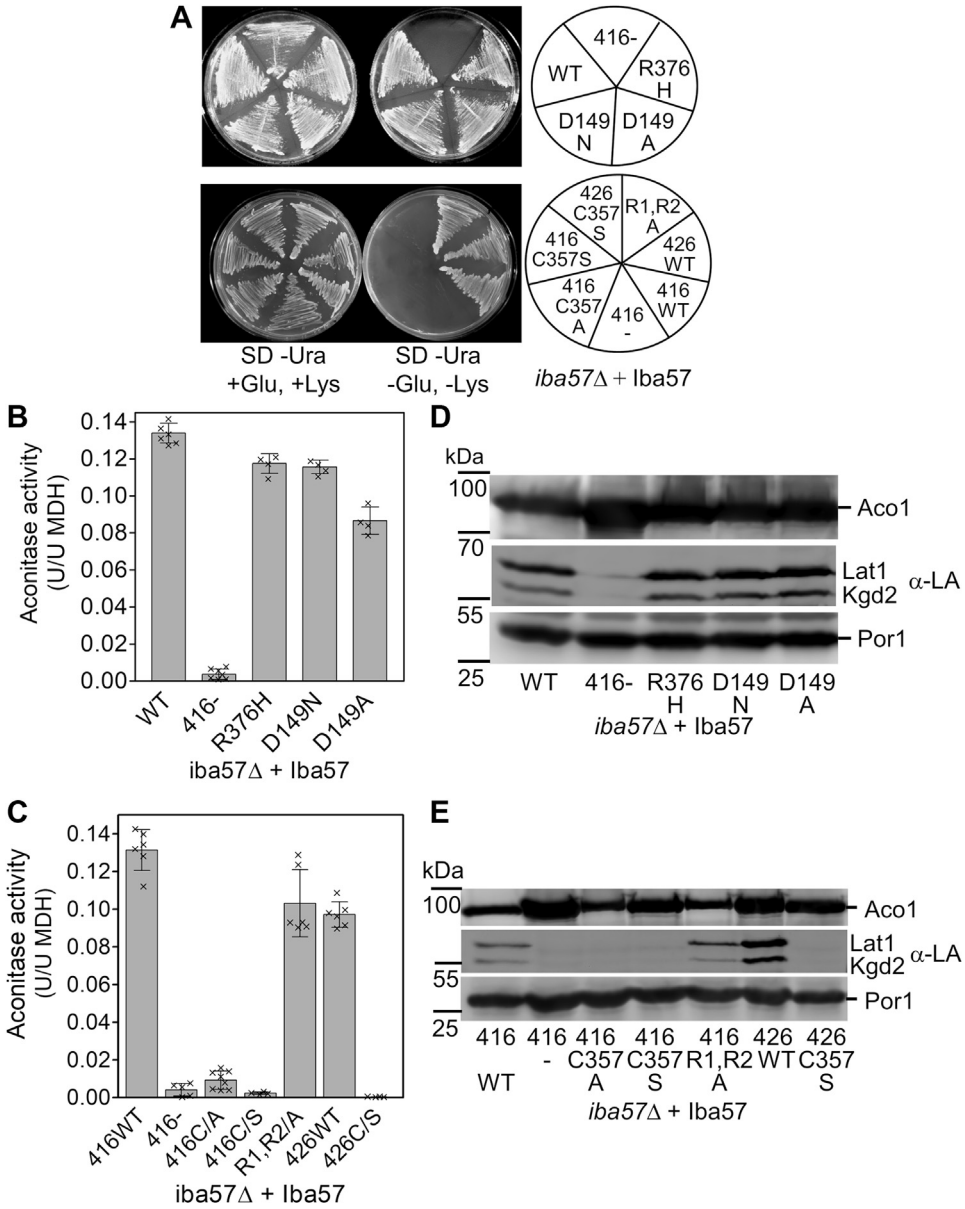

Figure 6. Potential THF-interacting residues are dispensable for *in vivo* function of Sclba57. *A,* yeast *iba57*Δ cells expressing either wildtype (WT) Sclba57 or the indicated point mutation variants from a centromeric plasmid (p416) under the control of the endogenous *IBA57* promoter were cultivated on solid synthetic defined (SD) minimal medium in the presence or the absence of Lys and Glu. *iba57*Δ with an empty vector (416) served as control. Overproduction of the Sclba57–C357S variant in *iba57*Δ cells from a high-copy vector (p426) did not lead to high-copy suppression. *B* and *C,* cells cultivated in SD minimal medium plus Lys and Glu were assayed for aconitase enzyme activities (relative to malate dehydrogenase [MDH]). *D* and *E,* the presence of aconitase and the lipoylation (LA) of the E2 subunits of pyruvate (Lat1) and 2-ketoglutarate dehydrogenases (Kgd2) was determined by immunostaining of isolated mitochondrial extracts. A stain for mitochondrial Por1 served as a loading control. Error bars indicate the standard deviation (n ≥ 4). Sclba57, *Saccharomyces cerevisiae* Iba57; THF, tetrahydrofolate.

was overexpressed from the strong *TDH3* promoter in a high-copy vector. This lack of high-copy suppression demonstrates that residue Cys357 is fully indispensable for *in vivo* function. Together, these physiological and biochemical findings clearly rule out a THF-dependent catalytic function of ScIba57 and thus fully support the conclusions drawn from inspection of the two Iba57 crystal structures.

Discussion

In eukaryotes, the late-acting ISC factors Isa1, Isa2, and Iba57 play an essential role in mitochondrial [4Fe–4S] protein biogenesis, and their function may in principle be conserved in bacteria (25–28, 70). In tight cooperation, they catalyze the reductive fusion of [2Fe–2S] clusters provided by the early parts of the mitochondrial ISC system to a [4Fe–4S] cluster (24). The interplay of these three proteins and the precise mechanistic role of each of these mitochondrial ISC factors are poorly resolved to date. Iba57 and its bacterial homolog YgfZ belong to the COG0354 protein family of folate-binding proteins with structural similarities to the T-subunit GcvT of the glycine cleavage system (31, 44). On first glance, this suggests a THF-dependent enzymatic function for both Iba57 and YgfZ. Consistent with this idea, *E. coli* strains with defects in folate biosynthesis or with a deletion of ygfZ show a 40% lower

activity of MiaB, a radical SAM [4Fe–4S] protein involved in tRNA modification (45–47). Moreover, EcYgfZ binds folate derivatives *in vitro*, yet with rather low (millimolar range) affinity. Since EcYgfZ can be functionally replaced in *E. coli* by mitochondrial Iba57 from various organisms including yeast and plants, it was proposed that the supposed folate-requiring function of EcYgfZ in the biogenesis of [4Fe–4S] proteins is generally conserved in mitochondrial Iba57 relatives. Yet, our genetic, mutational, biochemical, and structural studies refute a folate-dependent function of Iba57 (for discussion of YgfZ, see later). We provide three independent lines of evidence for this conclusion: (i) the lack of folate requirement for mitochondrial [4Fe–4S] protein maturation, (ii) the absence of a characteristic THF-binding pocket in Iba57 structures, and (iii) the inconspicuous phenotype of mutations of conserved Iba57 residues that are important for THF binding and THF-dependent catalysis in GcvT.

Our investigations of *S. cerevisiae* folate synthesis mutants (that can be complemented by the four folate-requiring metabolites, that is, adenine, His, Met, and dTMP (49–51)), revealed no folate requirement for the activities of mitochondrial [4Fe–4S] enzymes such as aconitase and lipoyl synthase, two key mitochondrial Fe–S proteins whose maturation strictly depends on Iba57 (25). This finding suggested no general involvement of folate in Iba57 function. Moreover, our folate synthesis mutants showed no auxotrophies for the two amino acids Lys and Glu that require mitochondrial [4Fe–4S] aconitase and homoaconitase for their synthesis. These requirements are characteristic genetic hallmarks of yeast cells deficient in Iba57, Isa1, or Isa2 (25, 26). Furthermore, our observations are fully consistent with earlier studies on folate-deficient yeast mutants that did not document any Lys or Glu requirements (48–52). Hence, our conclusion that folate does not play a role in mitochondrial [4Fe–4S] protein metabolism is fully in line with the available knowledge of folate and one-carbon metabolism in *S. cerevisiae*.

The crystal structures of both HsIBA57 and *C. thermophilum* Iba57 display an overall high structural similarity to THF-binding proteins including HsGcvT of the glycine cleavage system. Nevertheless, closer inspection of the Iba57 structures revealed several important differences that are incompatible with THF binding to Iba57. In both Iba57 proteins, the THF entry tunnel is blocked by two loops that have moved substantially from their original position in HsGcvT toward each other in Iba57. Furthermore, the THF-binding pocket is constricted and appears too small for accommodation of a folate molecule. More importantly, key residues that specifically coordinate the THF molecule in the HsGcvT-binding pocket are either absent in the Iba57 structures or are exchanged from charged to hydrophobic amino acids and vice versa. In Iba57, these nonconservative amino acid replacements are frequently shifted in position and point slightly away from the putative THF partner. As the only notable exception, the catalytically essential Asp101 of the THF-binding pocket of HsGcvT is fully conserved in Iba57 proteins (56, 60), yet, as discussed later, is not essential for yeast Iba57 function. Finally, the basic surface area that binds the polyglutamyl tail of THF and enhances THF binding in GcvT proteins is virtually absent in mitochondrial Iba57 structures. In eukaryotes, this tail is required for retention of THF in mitochondria and cytosol (52, 65, 68). In contrast, the lipoyl tunnel of GcvT that accommodates this cofactor attached to the GCSH subunit of the glycine-cleavage complex is maintained in Iba57 (57), yet many of the residues lining the tunnel are exchanged, rendering lipoyl binding unlikely. Consistently, no interaction between GCSH and Iba57 proteins is known (see, *e.g.*, (30)). Taken together, our structural analyses indicate that mitochondrial Iba57 has evolved into a THF-independent protein by altering the canonical THF-binding cavity of common GcvT-like precursors into a filled region. As a result, the Iba57 structures strongly argue against a THF-dependent function in mitochondrial [4Fe–4S] cluster formation. The functional role of the remnant THF domain, if any, remains to be determined.

A THF-independent function of mitochondrial Iba57 proteins is further made unlikely by mutational studies *in vivo*. THF-dependent one-carbon transfer reactions catalyzed by amino-methyltransferase GcvT (56, 59, 60), dimethylglycine oxidase DMGO (63), or guanine nucleotide-binding protein TrmE (64) essentially involve a strictly conserved aspartate residue (Asp101 in HsGcvT) that transiently forms a hydrogen bond with the catalytically important N10 group of THF. Asp101 assists the nucleophilic attack of the catalytic N10 group of THF on the methylene carbon on the lipoyl arm by proton abstraction. The corresponding aspartate in mitochondrial Iba57 is fully conserved. Yet, while exchanges of this residue in HsGcvT result in complete loss of enzymatic function *in vitro* (56), this residue is dispensable for Iba57 function *in vivo*, as indicated by inconspicuous growth phenotypes and wildtype Fe–S protein maturation activities. Furthermore, several other residues, which in HsGcvT interact with THF and upon exchange impair its function (56), are nonessential for Iba57 function, altogether excluding a THF-dependent enzymatic role. This conclusion is corroborated by *in vitro* findings showing that HsIBA57 is fully functional in [4Fe–4S] cluster maturation of aconitase without folate supplementation (24). Collectively, several independent functional and structural approaches suggest that mitochondrial Iba57, unlike its THF-dependent protein relatives, does not make use of folates for its function in mitochondrial [4Fe–4S] protein biogenesis.

Iba57 and YgfZ perform a shared function in [4Fe–4S] protein maturation as indicated by the complementation of an EcYgfZ deletion mutant by various mitochondrial Iba57 members (45, 47). Conversely, as shown here, EcYgfZ could not replace Iba57 function in yeast, clearly documenting differences between these proteins. A major difference between Iba57 and EcYgfZ appears to be their respective substrate spectrum. While Iba57 is indispensable for maturation of virtually all mitochondrial [4Fe–4S] proteins in yeast and humans, deletion of *ygfZ* in *E. coli* mainly affects the activity of the molybdopterin-containing dimethyl sulfoxide reductase (98% reduction; (25, 28, 45, 47, 71, 72)). Formation of the MiaB product 5-methylaminomethyl-2-thiouridine (mnm5s2U) as well as succinate dehydrogenase and fumarase activities are impaired by only ∼40%, whereas other Fe–S protein activities such as those of aconitase and sulfite reductase are even

increased upon *ygfZ* deletion (45). The broad and narrow substrate specificities of Iba57 and EcYgfZ, respectively, are well reflected by the fact that deletion of *ygfZ* in *E. coli* is not lethal, unlike that of the *ISA1* homolog *erpA*, encoding the potential EcYgfZ partner protein (73). A further distinction between Iba57 and EcYgfZ concerns the immediate partner proteins. Mitochondrial Iba57 has gained a binding partner, namely the A-type ISC factor Isa2, that has no known functional counterpart in bacteria (25, 30, 31). None of the three bacterial A-type ISC proteins IscA, SufA, or ErpA can functionally replace Isa2 in yeast, in contrast to Isa1 (26). Together, these genetic features document the profound phenotypical differences of mitochondrial Iba57 and bacterial YgfZ proteins, despite some basic functional overlap.

Can a different folate dependence of Iba57 and EcYgfZ proteins provide an explanation for these differences? So far, a folate requirement for Fe–S protein maturation in *E. coli* has been reported only for MiaB (45). *E. coli* folate mutants showed a ∼30% lower MiaB product formation compared with wildtype bacteria, similar to what was found for a *ygfZ* deletion mutant (see aforementioned). This rather weak defect indicates that folate is not essential for MiaB Fe-S cluster assembly and/or function. Moreover, our comparative structural analyses of both the putative THF-binding pocket and the lipoyl channel of EcYgfZ compared with those present in HsGcvT identify conspicuous differences. Even though in EcYgfZ, the THF-binding pocket may still be large enough to accommodate a THF molecule and the THF entry tunnel is still partially open, many of the specific THF-coordinating residues within the binding pocket are altered in a way making THF binding unlikely. Moreover, the Asp101 residue that is essential for THF-dependent catalysis in HsGcvT is mutated, and the positively charged surface required for interaction with the THF polyglutamyl tail is virtually missing. The lipoyl tunnel is even completely absent in EcYgfZ clearly excluding a binding of this cofactor. Collectively, the maintenance of a cavity in EcYgfZ is in principle compatible with THF binding, yet the largely altered biochemical environment of the putative THF-binding pocket renders stable THF binding and THF-dependent catalysis as seen in GcvT unlikely. Overall, this is consistent with the observed weak binding of THF to EcYgfZ in the millimolar range *in vitro* (44, 45) and explains why the cofactor was neither coisolated with the protein nor present in the crystal structures, as found for HsGcvT. These considerations may make it necessary to reinspect the THF requirement of bacterial Fe–S protein biogenesis in general and the impact of THF binding for YgfZ function in particular. Taken together, our structural analyses suggest that mitochondrial Iba57 and likely also bacterial YgfZ do not require THF to execute their partially shared function in [4Fe–4S] cluster formation.

Experimental procedures

Strains, growth conditions, and recombinant proteins

Yeast strains (Table S2) were cultivated in synthetic complete minimal medium supplemented with the required amino acids, 2% (w/v) carbon source and, when required, 100 μg/ml folic acid or 100 μg/ml dTMP (74). Plasmids are compiled in Table S3. For purification of recombinant CtIba57, the open reading frame of CtIba57 (codons 61–476) was fused to an N-terminal HIS tag in vector pRSFduet1. *E. coli* Bl21(DE3) cells were grown in LB medium at 37 °C to an absorbance of 0.5 at 600 nm. Protein expression was induced with IPTG (1 mM final), and cells were cultivated overnight at 28 °C. CtIBA57 was purified by nickel–nitrilotriacetic acid chromatography followed by gel filtration on a Superdex S200 column in buffer P (50 mM Tris–HCl, pH 8.0, 150 mM NaCl, and 5% glycerol).

Crystal structure of recombinant CtIba57

CtIba57 was concentrated to 35 mg/ml and crystallized in 0.1 M citric acid (pH 4.0) and 5% (w/v) PEG 6000 after 40 to 60 days incubation at ambient temperature. Crystals were flash frozen in liquid nitrogen employing a cryosolution that consisted of mother liquor supplemented with 30% (v/v) glycerol. Data were collected under cryogenic conditions at the European Synchrotron Radiation Facility at ID29. The crystal structure of CtIba57 (PDB code: 7Z3H) was solved by molecular replacement using the structure of the HsIBA57 (PDB code: 6QE4) as search model (Table S1, (31)).

Miscellaneous methods

Statistical analyses were carried out with GraphPad Prism 3 (GraphPad Software, Inc). Errors bars indicate the SEM. The following published methods were used: manipulation of DNA and PCR (75), transformation of yeast cells (76), preparation of yeast mitochondria and cell extracts (77), immunological techniques (78), and determination of enzyme activities in cell extracts (79).

Data availability

All data are contained within the article and the accompanying supporting information.

Supporting information—This article contains supporting information (24–26, 56, 76, 81–86).

Acknowledgments—We thank Devid Mrusek for help during crystallization of CtIBA57. We acknowledge the contribution of the Core Facility "Protein Biochemistry and Spectroscopy" of Philipps-Universität Marburg.

Author contributions—U. M. conceptualization; U. M. methodology; U. M., B. D. W., F. N., R. M., I. K., and F. A. investigation; U. M. writing–original draft; R. L. writing–review & editing; S.-A. F. and F. A. visualization; G. B. and R. L. supervision; R. L. project administration; R. L. funding acquisition.

Funding and additional information—The work was financially supported by Deutsche Forschungsgemeinschaft through funds from SFB 987 (to R.L. and U.M.) and SPPs 1710 and 1927 (to R.L.).

Conflict of interest—The authors declare that they have no conflicts of interest with the contents of this article.

Abbreviations—The abbreviations used are: CtIba57, *Chaetomium thermophilum* Iba57; dTMP, deoxythymidine monophosphate; EcYgfZ, *Escherichia coli* YgfZ; Fe-S, iron–sulfur; HsGcvT, human GcvT; HsIBA57, human IBA57; ISC, iron–sulfur cluster assembly; PDB, protein data bank; THF, tetrahydrofolate.

References

1. Zanello, P. (2019) Structure and electrochemistry of proteins harboring iron-sulfur clusters of different nuclearities. Part IV. Canonical, non-canonical and hybrid iron-sulfur proteins. *J. Struct. Biol.* **205**, 103–120
2. Braymer, J. J., Freibert, S. A., Rakwalska-Bange, M., and Lill, R. (2021) Mechanistic concepts of iron-sulfur protein biogenesis in biology. *Biochim. Biophys. Acta Mol. Cell Res* **1868**, 118863
3. Lill, R., and Freibert, S. A. (2020) Mechanisms of mitochondrial iron-sulfur protein biogenesis. *Annu. Rev. Biochem.* **89**, 471–499
4. Maio, N., Jain, A., and Rouault, T. A. (2020) Mammalian iron-sulfur cluster biogenesis: recent insights into the roles of frataxin, acyl carrier protein and ATPase-mediated transfer to recipient proteins. *Curr. Opin. Chem. Biol.* **55**, 34–44
5. Ciofi-Baffoni, S., Nasta, V., and Banci, L. (2018) Protein networks in the maturation of human iron-sulfur proteins. *Metallomics* **10**, 49–72
6. Przybyla-Toscano, J., Roland, M., Gaymard, F., Couturier, J., and Rouhier, N. (2018) Roles and maturation of iron-sulfur proteins in plastids. *J. Biol. Inorg. Chem.* **23**, 545–566
7. Baussier, C., Fakroun, S., Aubert, C., Dubrac, S., Mandin, P., Py, B., *et al.* (2020) Making iron-sulfur cluster: Structure, regulation and evolution of the bacterial ISC system. *Adv. Microb. Physiol.* **76**, 1–39
8. Freibert, S. A., Goldberg, A. V., Hacker, C., Molik, S., Dean, P., Williams, T. A., *et al.* (2017) Evolutionary conservation and *in vitro* reconstitution of microsporidian iron-sulfur cluster biosynthesis. *Nat. Commun.* **8**, 13932
9. Paul, V. D., and Lill, R. (2015) Biogenesis of cytosolic and nuclear iron-sulfur proteins and their role in genome stability. *Biochim. Biophys. Acta* **1853**, 1528–1539
10. Parent, A., Elduque, X., Cornu, D., Belot, L., Le Caer, J. P., Grandas, A., *et al.* (2015) Mammalian frataxin directly enhances sulfur transfer of NFS1 persulfide to both ISCU and free thiols. *Nat. Commun.* **6**, 5686
11. Webert, H., Freibert, S. A., Gallo, A., Heidenreich, T., Linne, U., Amlacher, S., *et al.* (2014) Functional reconstitution of mitochondrial Fe/S cluster synthesis on Isu1 reveals the involvement of ferredoxin. *Nat. Commun.* **5**, 5013
12. Boniecki, M. T., Freibert, S. A., Muhlenhoff, U., Lill, R., and Cygler, M. (2017) Structure and functional dynamics of the mitochondrial Fe/S cluster synthesis complex. *Nat. Commun.* **8**, 1287
13. Gervason, S., Larkem, D., Mansour, A. B., Botzanowski, T., Muller, C. S., Pecqueur, L., *et al.* (2019) Physiologically relevant reconstitution of iron-sulfur cluster biosynthesis uncovers persulfide-processing functions of ferredoxin-2 and frataxin. *Nat. Commun.* **10**, 3566
14. Muhlenhoff, U., Gerber, J., Richhardt, N., and Lill, R. (2003) Components involved in assembly and dislocation of iron-sulfur clusters on the scaffold protein Isu1p. *Embo J.* **22**, 4815–4825
15. Kim, J. H., Frederick, R. O., Reinen, N. M., Troupis, A. T., and Markley, J. L. (2013) [2Fe-2S]-ferredoxin binds directly to cysteine desulfurase and supplies an electron for iron-sulfur cluster assembly but is displaced by the scaffold protein or bacterial frataxin. *J. Am. Chem. Soc.* **135**, 8117–8120
16. Freibert, S. A., Boniecki, M. T., Stumpfig, C., Schulz, V., Krapoth, N., Winge, D. R., *et al.* (2021) N-terminal tyrosine of ISCU2 triggers [2Fe-2S] cluster synthesis by ISCU2 dimerization. *Nat. Commun.* **12**, 6902
17. Kampinga, H. H., and Craig, E. A. (2010) The HSP70 chaperone machinery: j proteins as drivers of functional specificity. *Nat. Rev. Mol. Cell Biol* **11**, 579–592
18. Dutkiewicz, R., and Nowak, M. (2018) Molecular chaperones involved in mitochondrial iron-sulfur protein biogenesis. *J. Biol. Inorg. Chem.* **23**, 569–579
19. Dutkiewicz, R., Nowak, M., Craig, E. A., and Marszalek, J. (2017) Fe-S cluster Hsp70 chaperones: the ATPase cycle and protein interactions. *Methods Enzymol.* **595**, 161–184
20. Kleczewska, M., Grabinska, A., Jelen, M., Stolarska, M., Schilke, B., Marszalek, J., *et al.* (2020) Biochemical convergence of mitochondrial Hsp70 system specialized in iron-sulfur cluster biogenesis. *Int. J. Mol. Sci.* **21**
21. Berndt, C., Christ, L., Rouhier, N., and Muhlenhoff, U. (2021) Glutaredoxins with iron-sulphur clusters in eukaryotes - structure, function and impact on disease. *Biochim. Biophys. Acta Bioenerg.* **1862**, 148317
22. Banci, L., Brancaccio, D., Ciofi-Baffoni, S., Del Conte, R., Gadepalli, R., Mikolajczyk, M., *et al.* (2014) [2Fe-2S] cluster transfer in iron-sulfur protein biogenesis. *Proc. Natl. Acad. Sci. U S A.* **111**, 6203–6208
23. Trnka, D., Engelke, A. D., Gellert, M., Moseler, A., Hossain, M. F., Lindenberg, T. T., *et al.* (2020) Molecular basis for the distinct functions of redox-active and FeS-transfering glutaredoxins. *Nat. Commun.* **11**, 3445
24. Weiler, B. D., Bruck, M. C., Kothe, I., Bill, E., Lill, R., and Muhlenhoff, U. (2020) Mitochondrial [4Fe-4S] protein assembly involves reductive [2Fe-2S] cluster fusion on ISCA1-ISCA2 by electron flow from ferredoxin FDX2. *Proc. Natl. Acad. Sci. U. S. A.* **117**, 20555–20565
25. Gelling, C., Dawes, I. W., Richhardt, N., Lill, R., and Muhlenhoff, U. (2008) Mitochondrial Iba57p is required for Fe/S cluster formation on aconitase and activation of radical SAM enzymes. *Mol. Cell Biol* **28**, 1851–1861
26. Muhlenhoff, U., Richter, N., Pines, O., Pierik, A. J., and Lill, R. (2011) Specialized function of yeast Isa1 and Isa2 proteins in the maturation of mitochondrial [4Fe-4S] proteins. *J. Biol. Chem.* **286**, 41205–41216
27. Long, S., Changmai, P., Tsaousis, A. D., Skalicky, T., Verner, Z., Wen, Y. Z., *et al.* (2011) Stage-specific requirement for Isa1 and Isa2 proteins in the mitochondrion of Trypanosoma brucei and heterologous rescue by human and blastocystis orthologues. *Mol. Microbiol.* **81**, 1403–1418
28. Sheftel, A. D., Wilbrecht, C., Stehling, O., Niggemeyer, B., Elsasser, H. P., Muhlenhoff, U., *et al.* (2012) The human mitochondrial ISCA1, ISCA2, and IBA57 proteins are required for [4Fe-4S] protein maturation. *Mol. Biol. Cell* **23**, 1157–1166
29. Brancaccio, D., Gallo, A., Mikolajczyk, M., Zovo, K., Palumaa, P., Novellino, E., *et al.* (2014) Formation of [4Fe-4S] clusters in the mitochondrial iron-sulfur cluster assembly machinery. *J. Am. Chem. Soc.* **136**, 16240–16250
30. Beilschmidt, L. K., Ollagnier de Choudens, S., Fournier, M., Sanakis, I., Hograindleur, M. A., Clemancey, M., *et al.* (2017) ISCA1 is essential for mitochondrial Fe4S4 biogenesis *in vivo*. *Nat. Commun.* **8**, 15124
31. Gourdoupis, S., Nasta, V., Calderone, V., Ciofi-Baffoni, S., and Banci, L. (2018) IBA57 recruits ISCA2 to form a [2Fe-2S] cluster-mediated complex. *J. Am. Chem. Soc.* **140**, 14401–14412
32. Nasta, V., Da Vela, S., Gourdoupis, S., Ciofi-Baffoni, S., Svergun, D. I., and Banci, L. (2019) Structural properties of [2Fe-2S] ISCA2-IBA57: A complex of the mitochondrial iron-sulfur cluster assembly machinery. *Sci. Rep.* **9**, 18986
33. Nasta, V., Suraci, D., Gourdoupis, S., Ciofi-Baffoni, S., and Banci, L. (2020) A pathway for assembling [4Fe-4S](2+) clusters in mitochondrial iron-sulfur protein biogenesis. *Febs J.* **287**, 2312–2327
34. Bych, K., Kerscher, S., Netz, D. J., Pierik, A. J., Zwicker, K., Huynen, M. A., *et al.* (2008) The iron-sulphur protein Ind1 is required for effective complex I assembly. *Embo J.* **27**, 1736–1746
35. Melber, A., Na, U., Vashisht, A., Weiler, B. D., Lill, R., Wohlschlegel, J. A., *et al.* (2016) Role of Nfu1 and Bol3 in iron-sulfur cluster transfer to mitochondrial clients. *eLife* **5**
36. Uzarska, M. A., Nasta, V., Weiler, B. D., Spantgar, F., Ciofi-Baffoni, S., Saviello, M. R., *et al.* (2016) Mitochondrial Bol1 and Bol3 function as assembly factors for specific iron-sulfur proteins. *eLife* **5**
37. Navarro-Sastre, A., Tort, F., Stehling, O., Uzarska, M. A., Arranz, J. A., Del Toro, M., *et al.* (2011) A fatal mitochondrial disease is associated with defective NFU1 function in the maturation of a subset of mitochondrial Fe-S proteins. *Am. J. Hum. Genet.* **89**, 656–667
38. Cameron, J. M., Janer, A., Levandovskiy, V., Mackay, N., Rouault, T. A., Tong, W. H., *et al.* (2011) Mutations in iron-sulfur cluster scaffold genes

NFU1 and BOLA3 cause a fatal deficiency of multiple respiratory chain and 2-oxoacid dehydrogenase enzymes. *Am. J. Hum. Genet.* **89**, 486–495
39. Ajit Bolar, N., Vanlander, A. V., Wilbrecht, C., Van der Aa, N., Smet, J., De Paepe, B., *et al.* (2013) Mutation of the iron-sulfur cluster assembly gene IBA57 causes severe myopathy and encephalopathy. *Hum. Mol. Genet.* **22**, 2590–2602
40. Al-Hassnan, Z. N., Al-Dosary, M., Alfadhel, M., Faqeih, E. A., Alsagob, M., Kenana, R., *et al.* (2015) ISCA2 mutation causes infantile neurodegenerative mitochondrial disorder. *J. Med. Genet.* **52**, 186–194
41. Torraco, A., Stehling, O., Stumpfig, C., Rosser, R., De Rasmo, D., Fiermonte, G., *et al.* (2018) ISCA1 mutation in a patient with infantile-onset leukodystrophy causes defects in mitochondrial [4Fe-4S] proteins. *Hum. Mol. Genet.* **27**, 2739–2754
42. Stehling, O., Paul, V. D., Bergmann, J., Basu, S., and Lill, R. (2018) Biochemical analyses of human iron-sulfur protein biogenesis and of related diseases. *Methods Enzymol.* **599**, 227–263
43. Lebigot, E., Schiff, M., and Golinelli-Cohen, M. P. (2021) A Review of multiple mitochondrial dysfunction syndromes, syndromes associated with defective Fe-S protein maturation. *Biomedicines* **9**
44. Teplyakov, A., Obmolova, G., Sarikaya, E., Pullalarevu, S., Krajewski, W., Galkin, A., *et al.* (2004) Crystal structure of the YgfZ protein from Escherichia coli suggests a folate-dependent regulatory role in one-carbon metabolism. *J. Bacteriol.* **186**, 7134–7140
45. Waller, J. C., Alvarez, S., Naponelli, V., Lara-Nunez, A., Blaby, I. K., Da Silva, V., *et al.* (2010) A role for tetrahydrofolates in the metabolism of iron-sulfur clusters in all domains of life. *Proc. Natl. Acad. Sci. U. S. A.* **107**, 10412–10417
46. Hasnain, G., Waller, J. C., Alvarez, S., Ravilious, G. E., Jez, J. M., and Hanson, A. D. (2012) Mutational analysis of YgfZ, a folate-dependent protein implicated in iron/sulphur cluster metabolism. *FEMS Microbiol. Lett.* **326**, 168–172
47. Waller, J. C., Ellens, K. W., Alvarez, S., Loizeau, K., Ravanel, S., and Hanson, A. D. (2012) Mitochondrial and plastidial COG0354 proteins have folate-dependent functions in iron-sulphur cluster metabolism. *J. Exp. Bot.* **63**, 403–411
48. Zheng, Y., and Cantley, L. C. (2019) Toward a better understanding of folate metabolism in health and disease. *J. Exp. Med.* **216**, 253–266
49. Bayly, A. M., Berglez, J. M., Patel, O., Castelli, L. A., Hankins, E. G., Coloe, P., *et al.* (2001) Folic acid utilisation related to sulfa drug resistance in Saccharomyces cerevisiae. *FEMS Microbiol. Lett.* **204**, 387–390
50. Christensen, K. E., and MacKenzie, R. E. (2006) Mitochondrial one-carbon metabolism is adapted to the specific needs of yeast, plants and mammals. *Bioessays* **28**, 595–605
51. Locasale, J. W. (2013) Serine, glycine and one-carbon units: Cancer metabolism in full circle. *Nat. Rev. Cancer* **13**, 572–583
52. Cherest, H., Thomas, D., and Surdin-Kerjan, Y. (2000) Polyglutamylation of folate coenzymes is necessary for methionine biosynthesis and maintenance of intact mitochondrial genome in Saccharomyces cerevisiae. *J. Biol. Chem.* **275**, 14056–14063
53. Garavaglia, B., Invernizzi, F., Carbone, M. L., Viscardi, V., Saracino, F., Ghezzi, D., *et al.* (2004) GTP-Cyclohydrolase I gene mutations in patients with autosomal dominant and recessive GTP-CH1 deficiency: Identification and functional characterization of four novel mutations. *J. Inherit. Metab. Dis.* **27**, 455–463
54. Cai, C., Shi, W., Zeng, Z., Zhang, M., Ling, C., Chen, L., *et al.* (2013) GTP cyclohydrolase I and tyrosine hydroxylase gene mutations in familial and sporadic dopa-responsive dystonia patients. *PLoS One* **8**, e65215
55. Uzarska, M. A., Przybyla-Toscano, J., Spantgar, F., Zannini, F., Lill, R., Muhlenhoff, U., *et al.* (2018) Conserved functions of Arabidopsis mitochondrial late-acting maturation factors in the trafficking of iron sulfur clusters. *Biochim. Biophys. Acta Mol. Cell Res* **1865**, 1250–1259
56. Okamura-Ikeda, K., Hosaka, H., Yoshimura, M., Yamashita, E., Toma, S., Nakagawa, A., *et al.* (2005) Crystal structure of human T-protein of glycine cleavage system at 2.0 A resolution and its implication for understanding non-ketotic hyperglycinemia. *J. Mol. Biol.* **351**, 1146–1159
57. Okamura-Ikeda, K., Hosaka, H., Maita, N., Fujiwara, K., Yoshizawa, A. C., Nakagawa, A., *et al.* (2010) Crystal structure of aminomethyltransferase in complex with dihydrolipoyl-H-protein of the glycine cleavage system: Implications for recognition of lipoyl protein substrate, disease-related mutations, and reaction mechanism. *J. Biol. Chem.* **285**, 18684–18692
58. Kikuchi, G., Motokawa, Y., Yoshida, T., and Hiraga, K. (2008) Glycine cleavage system: Reaction mechanism, physiological significance, and hyperglycinemia. *Proc. Jpn. Acad. Ser. B Phys. Biol. Sci.* **84**, 246–263
59. Lokanath, N. K., Kuroishi, C., Okazaki, N., and Kunishima, N. (2005) Crystal structure of a component of glycine cleavage system: T-Protein from pyrococcus horikoshii OT3 at 1.5 A resolution. *Proteins* **58**, 769–773
60. Lee, H. H., Kim, D. J., Ahn, H. J., Ha, J. Y., and Suh, S. W. (2004) Crystal structure of T-protein of the glycine cleavage system. Cofactor binding, insights into H-protein recognition, and molecular basis for understanding nonketotic hyperglycinemia. *J. Biol. Chem.* **279**, 50514–50523
61. Orun, O., Koch, M. H., Kan, B., Svergun, D. I., Petoukhov, M. V., and Sayers, Z. (2003) Structural characterization of T-protein of the Escherichia coli glycine cleavage system by X-ray small angle scattering. *Cell Mol Biol (Noisy-le-grand)* **49**, OL453–OL459
62. Scrutton, N. S., and Leys, D. (2005) Crystal structure of DMGO provides a prototype for a new tetrahydrofolate-binding fold. *Biochem. Soc. Trans.* **33**, 776–779
63. Leys, D., Basran, J., and Scrutton, N. S. (2003) Channelling and formation of 'active' formaldehyde in dimethylglycine oxidase. *Embo J.* **22**, 4038–4048
64. Scrima, A., Vetter, I. R., Armengod, M. E., and Wittinghofer, A. (2005) The structure of the TrmE GTP-binding protein and its implications for tRNA modification. *Embo J.* **24**, 23–33
65. Raz, S., Stark, M., and Assaraf, Y. G. (2016) Folylpoly-gamma-glutamate synthetase: a key determinant of folate homeostasis and antifolate resistance in cancer. *Drug Resist Update* **28**, 43–64
66. Osborne, C. B., Lowe, K. E., and Shane, B. (1993) Regulation of folate and one-carbon metabolism in mammalian-cells .1. Folate metabolism in Chinese-hamster ovary cells expressing escherichia-coli or human folylpoly-gamma-glutamate synthetase-activity. *J. Biol. Chem.* **268**, 21657–21664
67. Toone, J. R., Applegarth, D. A., Levy, H. L., Coulter-Mackie, M. B., and Lee, G. (2003) Molecular genetic and potential biochemical characteristics of patients with T-protein deficiency as a cause of glycine encephalopathy (NKH). *Mol. Genet. Metab.* **79**, 272–280
68. Lawrence, S. A., Titus, S. A, Ferguson, J., Heineman, A. L., Taylor, S. M., and Moran, R. G. (2014) Mammalian mitochondrial and cytosolic folylpolyglutamate synthetase maintain the subcellular compartmentalization of folates. *J. Biol. Chem.* **289**, 29386–29396
69. Lin, C. N., Syu, W. J., Sun, W. S., Chen, J. W., Chen, T. H., Don, M. J., *et al.* (2010) A role of ygfZ in the Escherichia coli response to plumbagin challenge. *J. Biomed. Sci.* **17**, 84
70. Py, B., Gerez, C., Huguenot, A., Vidaud, C., Fontecave, M., Ollagnier de Choudens, S., *et al.* (2018) The ErpA/NfuA complex builds an oxidation-resistant Fe-S cluster delivery pathway. *J. Biol. Chem.* **293**, 7689–7702
71. Waller, J. C., Ellens, K. W., Hasnain, G., Alvarez, S., Rocca, J. R., and Hanson, A. D. (2012) Evidence that the folate-dependent proteins YgfZ and MnmEG have opposing effects on growth and on activity of the iron-sulfur enzyme MiaB. *J. Bacteriol.* **194**, 362–367
72. Yu, H., and Kim, K. S. (2012) YgfZ contributes to secretion of cytotoxic necrotizing factor 1 into outer-membrane vesicles in Escherichia coli. *Microbiology (Reading)* **158**, 612–621
73. Loiseau, L., Gerez, C., Bekker, M., Ollagnier-de Choudens, S., Py, B., Sanakis, Y., *et al.* (2007) ErpA, an iron sulfur (Fe S) protein of the A-type essential for respiratory metabolism in Escherichia coli. *Proc. Natl. Acad. Sci. U. S. A.* **104**, 13626–13631
74. Sherman, F. (2002) Getting started with yeast. *Methods Enzymol.* **350**, 3–41
75. Sambrook, J., and Russel, D. W. (2001) *Molecular Cloning - A Laboratory Manual*, 3rd ed., CSH Laboratory Press, ColdSpring Harbour, NY
76. Gietz, R. D., and Woods, R. A. (2002) Transformation of yeast by lithium acetate/single-stranded carrier DNA/polyethylene glycol method. *Methods Enzymol.* **350**, 87–96

77. Diekert, K., de Kroon, A. I., Kispal, G., and Lill, R. (2001) Isolation and subfractionation of mitochondria from the yeast Saccharomyces cerevisiae. *Methods Cell Biol.* **65**, 37–51
78. Greenfield, E. A. (2012) *Antibodies - A Laboratory Manual*, 2nd ed., CSH Laboratory Press, Cold Spring Harbour, NY
79. Molik, S., Lill, R., and Muhlenhoff, U. (2007) Methods for studying iron metabolism in yeast mitochondria. *Methods Cell Biol.* **80**, 261–280
80. Jurrus, E., Engel, D., Star, K., Monson, K., Brandi, J., Felberg, L. E., *et al.* (2018) Improvements to the APBS biomolecular solvation software suite. *Protein Sci.* **27**, 112–128
81. Mortimer, R. K., and Johnston, J. R. (1986) Genealogy of principal strains of the yeast genetic stock center. *Genetics* **113**, 35–43
82. Brachmann, C. B., Davies, A., Cost, G. J., Caputo, E., Li, J., Hieter, P., *et al.* (1998) Designer deletion strains derived from Saccharomyces cerevisiae S288C: a useful set of strains and plasmids for PCR-mediated gene disruption and other applications. *Yeast* **14**, 115–132
83. Janke, C., Magiera, M. M., Rathfelder, N., Taxis, C., Reber, S., Maekawa, H., *et al.* (2004) A versatile toolbox for PCR-based tagging of yeast genes: new fluorescent proteins, more markers and promoter substitution cassettes. *Yeast* **21**, 947–962
84. Gueldener, U., Heinisch, J., Koehler, G. J., Voss, D., and Hegemann, J. H. (2002) A second set of loxP marker cassettes for Cre-mediated multiple gene knockouts in budding yeast. *Nucleic Acids Res.* **30**, e23
85. Muhlenhoff, U., Richhardt, N., Ristow, M., Kispal, G., and Lill, R. (2002) The yeast frataxin homolog Yfh1p plays a specific role in the maturation of cellular Fe/S proteins. *Hum. Mol. Genet.* **11**, 2025–2036
86. Funk, M., Niedenthal, R., Mumberg, D., Brinkmann, K., Ronicke, V., and Henkel, T. (2002) Vector systems for heterologous expression of proteins in Saccharomyces cerevisiae. *Methods Enzymol.* **350**, 248–257